Bull. Mater. Sci. (2023)46:80
https://doi.org/10.1007/s12034-023-02919-1

High-efficiency dye-sensitized solar cells fabricated with electrospun PVdF-HFP polymer nanofibre-based gel electrolytes

M A K L DISSANAYAKE[1,2,*], M S H HETTIARACHCHI[1,2], G K R SENADEERA[1,3], J M K W KUMARI[1,2], K UMAIR[1,2], T M W J BANDARA[2,4], I ALBINSSON[5], M FURLANI[6], B-E MELLANDER[6], N B CHAURE[7] and O I OLUSOLA[8]

[1]National Institute of Fundamental Studies, Kandy 20000, Sri Lanka
[2]Postgraduate Institute of Science, University of Peradeniya, Peradeniya 20400, Sri Lanka
[3]Department of Physics, The Open University of Sri Lanka, Nawala, Nugegoda 10250, Sri Lanka
[4]Department of Physics, University of Peradeniya, Peradeniya 20400, Sri Lanka
[5]Department of Physics, University of Gothenburg, Gothenburg 41296, Sweden
[6]Department of Applied Physics, Chalmers University of Technology, Gothenburg 41296, Sweden
[7]Department of Physics, Savitribai Phule Pune University, Pune 411007, India
[8]Department of Physics, The Federal University of Technology Akure, Akure 340271, Nigeria
*Author for correspondence (makldis@yahoo.com)

MS received 20 August 2022; accepted 17 December 2022

Abstract. Poly(vinylidene fluoride-co-hexafluoropropylene) (PVdF-HFP) electrospun polymer nanofibre-based quasi-solid or gel electrolytes were successfully fabricated by incorporating a liquid electrolyte within the nanofibre membrane. The dye-sensitized solar cells (DSSCs) fabricated with gel and with liquid electrolyte were characterized by photocurrent–voltage measurements and electrochemical impedance spectroscopy measurements. The maximum efficiency (η) of 6.79% was observed for the DSSC fabricated with optimized nanofibre membrane thickness, corresponding to 4 min of electrospinning time. The optimized PVdF-HFP nanofibre gel electrolyte shows an ionic conductivity of 7.16×10^{-3} S cm^{-1} at 25°C, while the corresponding liquid electrolyte exhibits an ionic conductivity of 11.69×10^{-3} S cm^{-1} at the same temperature. The open circuit voltage (V_{oc}), short circuit current density (J_{sc}) and fill factor were recorded as 801.40 mV, 12.70 mA cm^{-2}, and 66.67%, respectively, at an incident light intensity of 100 mW cm^{-2} with a 1.5 AM filter. The nanofibre gel electrolyte-based cell showed an efficiency of 6.79%, whereas the efficiency of the conventional liquid electrolyte-based cell was 7.28% under the same conditions. Furthermore, nanofibre gel electrolyte-based cells exhibited better stability, maintaining 85.40% of initial efficiency after 120 h. These results show that the optimized, polymer nanofibre-based gel electrolyte can be used successfully to replace the liquid electrolyte in DSSCs without much loss of efficiency but improving the stability while minimizing most of the drawbacks associated with liquid electrolytes.

Keywords. Electrospinning; nanofibre gel polymer electrolyte; dye-sensitized solar cells; PVdF-HFP co-polymer.

1. Introduction

Nanotechnology is a revolutionary and ubiquitous technology, and the advancements in nanomaterials research have gained tremendous attention in modern science and technology due to their remarkable properties in biological, chemical, and physical aspects [1]. One-dimensional nanomaterials, such as nanofibres, nanowires, nanotubes and nanorods which are functionalized with flexible surface properties, have attracted extensive attention due to their unique characteristics [2]. Among these, polymer nanofibres have been the foremost focused studies because of their attractive properties such as the large surface area to volume ratio, flexibility in surface functionalities, higher aspect ratio, better pore interconnectivity and superior mechanical stability [3].

There are numerous methods to produce polymer nanofibres, such as drawing, template synthesis, phase separation, self-assembly, chemical vapor deposition, wet chemical synthesis and electrospinning [4]. However, the applicability of most of the methods has been limited according to the material type, cost and production rate. Therefore, physical approaches such as electrospinning are more advantageous and have a leading edge over all other techniques due to their ability to produce consistent fibres with versatility, simplicity, low cost and relatively high production rate. Electrospinning can be considered as a modification of the electrospraying process that relies on repulsive electrostatic forces to fabricate ultrafine nanofibres from polymer solutions or polymer melts [3]. Solar photovoltaic devices offer an attractive method for the utilization of solar energy as it can directly convert solar energy

Published online: 20 April 2023

into electricity. Though the methods of utilizing solar energy are simple, they need efficient and durable solar photovoltaic materials because the degradation, low stability and high manufacturing cost are serious concerns, especially in third-generation solar cells like dye-sensitized solar cells (DSSCs) [5]. O'Reagan and Gratzel first reported DSSCs in 1991, and they are emerging as the next-generation solar cells, which are being developed as potential replacements to the conventional single-crystalline Si solar cells owing to their higher efficiency, simpler production process, lower material cost and environmental friendliness [6].

DSSCs fabricated with conventional liquid electrolytes consisting of a triiodide/iodide redox couple in an organic solvent have exhibited impressive energy conversion efficiencies. However, the lack of long-term stability due to the volatility of the electrolyte, difficulty in robust sealing, liquid leakage, electrode corrosion and photodecomposition of the dye are some of the major drawbacks, which prevent the large-scale practical applications of DSSCs [7]. Therefore, many research studies are being carried out to replace liquid electrolytes with alternatives such as inorganic or organic hole conductors, ionic liquids, solid electrolytes and polymer gel electrolytes [8]. Even though DSSCs fabricated with solid electrolytes offer a possible solution by providing long-term stability, they have low efficiencies compared to their liquid electrolyte counterparts due to their poor electrode/electrolyte contacts. On the other hand, DSSCs made with conventional gel polymer electrolytes exhibit relatively higher efficiencies than solid or gel electrolyte-based cells, but their efficiencies are lower than their liquid counterparts [7, 9].

Recent studies have shown that DSSCs based on gel electrolytes made by trapping a solution electrolyte within a three-dimensional matrix made of polymer nanofibres offer higher conversion efficiencies close to that of their liquid counterparts, while marinating a good dimensional stability as well. In these nanofibre-based gel electrolytes, the liquid electrolyte is 'entrapped' within the host polymer matrix, which can be produced by techniques such as electrospinning and they exhibit almost liquid-like ionic conductivities, while offering better mechanical and chemical stability for the DSSCs [10]. A schematic diagram of a DSSC fabricated with a polymer nanofibre gel electrolyte is shown in figure 1.

The present study used polyvinylidene fluoride-co-hexafluoropropylene (PVdF-HFP) co-polymer to fabricate the nanofibre membrane due to its unique properties such as low glass transition temperature, high solubility for organic solvents, low crystallinity, high electrochemical stability and adequate resistance with electrolyte [7, 11].

2. Experimental

2.1 *Materials*

Commercial grade P25 nanopowder was purchased from Degussa, and P90 TiO_2 nanoparticles were purchased from Evonik, Germany. Ruthenium sensitizer dye di-tetrabutylammonium cis-bis(isothiocyanato)bis(2,2′-bipyridyl-4,4′ dicarboxylato) ruthenium (II) (N719) and fluorine-doped SnO_2 coated (FTO) glass (sheet resistance 8 Ω cm^{-2}, 3.0 mm thickness) were purchased from Solaronix Switzerland. *N,N*-dimethylformamide (DMF), and polyethylene glycol 2000 (PEG-2000) (1900–2200 Mw, 99.8%) were purchased from BDH organics. Ethylene carbonate (EC, 99%) and propylene carbonate (PC, 99%) were purchased from Fluka Analytical. Polyvinylidene fluoride-co-hexafluoropropylene (PVdF-HFP, Mw ∼ 400,000), iodine (I_2, 99.8%), tetrapropylammonium iodide (TPAI, 99%), potassium iodide (KI, 99%), 4-tert butylpyridine (TBP, 98%) and guanidinium thiocyanate (GuSCN, 99%) were purchased from Sigma-Aldrich.

2.2 *Preparation of the PVdF-HFP nanofibre membranes*

PVdF-HFP nanofibres were prepared using a commercially purchased electrospinning system (NaBond Technologies, Hong Kong). The electrospinning polymer solution was prepared from a solution of 11 wt% PVdF-HFP in DMF by magnetically stirring for overnight. The following electrospinning parameters were set after optimization. The tip-to-collector distance was fixed at 6.5 cm. DC voltage (12 kV) was applied between the spinneret and the drum collector, and the syringe pump flow rate was adjusted to 0.8 ml h^{-1}. The electrospun PVdF-HFP nanofibres were collected onto platinized glass plates attached to the drum collector, rotating at 800 rpm.

2.3 *Fabrication of quasi-solid-state DSSC*

In order to fabricate the dense, compact layer of TiO_2, 0.25 g of P90 TiO_2 powder was ground well with 1 ml of 0.1 M nitric acid in an agate mortar for 10 min. The prepared solution was spin coated on cleaned fluorine-doped tin oxide (FTO) glass substrates at 3000 rpm for 60 s. The coated glass plates were sintered at 450°C for 45 min and gradually cooled to room temperature. Next, in order to fabricate a porous TiO_2 layer, TiO_2 paste was prepared by grinding commercial 0.25 g of P25 TiO_2 powder with 1 ml of 0.1 M nitric acid, 0.02 g of triton X-100 and 0.05 g of PEG 2000 and was spread over the previously prepared P90 compact layer/FTO by doctor blade technique. Subsequently, it was sintered at 450°C for 45 min and allowed to cool down gradually to room temperature. Sintered plates, each having an area of 0.25 cm^2, were immersed in a 0.3 mM solution of N719 dye dissolved in ethanol for 24 h in order to obtain dye-sensitized bi-layer photoanodes. After the dye adsorption, each TiO_2 photoanode was rinsed with absolute ethanol and air-dried to remove any residual moisture.

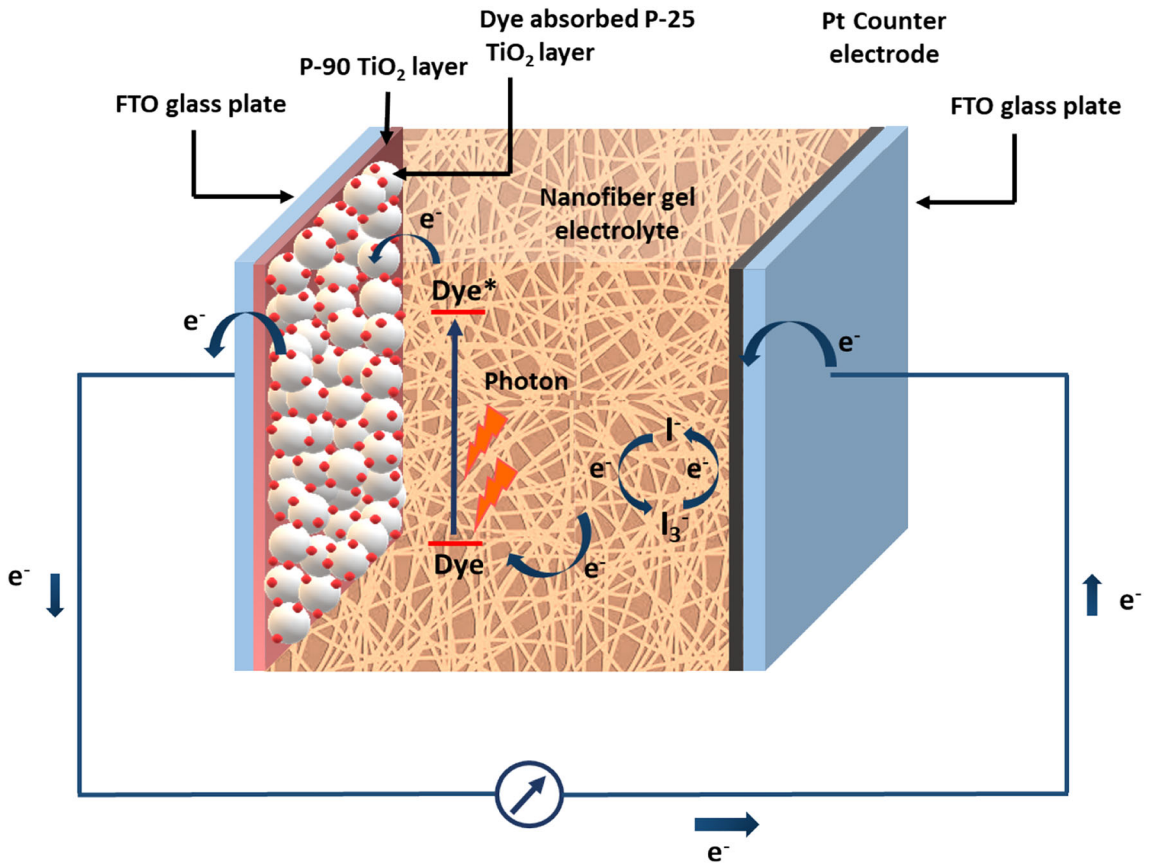

Figure 1. Schematic diagram of a DSSC fabricated with a polymer nanofibre gel electrolyte.

Based on previous studies carried out by our group [12], the acetonitrile-free electrolyte was prepared by dissolving 0.018 g of KI, 0.136 g of TPAI, 0.0166 g of I_2, 0.048 g of GuSCN and 75.52 µl of TBP in a mixture of PC (0.4 g) and EC (0.4 g). In order to obtain a homogeneous electrolyte, the solution was magnetically stirred overnight at room temperature in a tightly sealed glass bottle. Two drops of the liquid electrolyte were placed on the PVdF-HFP nanofibre deposited platinum plate and kept for 30 min to complete the adsorption of the electrolyte by the nanofibre membrane to form the quasi-solid-state (gel) electrolyte. The excess amount of the liquid electrolyte was gently wiped off using filter paper. The PVdF-HFP nanofibre gel electrolyte-incorporated DSSC was fabricated by keeping the dye-sensitized TiO_2 electrode on the nanofibre gel electrolyte to form the FTO/TiO_2/gel electrolyte/Pt sandwich structure using stainless steel clips under gentle pressure. For the comparative studies, a DSSC of configuration FTO/TiO_2/electrolyte/Pt was fabricated by sandwiching sufficient liquid electrolyte between the TiO_2 photoanode and the Pt counter electrode using stainless steel clips under gentle pressure. The dimension of each cell is 0.5 cm × 0.5 cm with an effective area of 0.25 cm^2.

2.4 *Characterization*

The surface morphology of the electrospun PVdF-HFP nanofibre membrane was examined using scanning electron microscopy (SEM, Zeiss). The photocurrent density *vs.* voltage (*J–V*) characteristics were measured under the illumination of 100 mW cm^{-2} (AM 1.5) simulated sunlight with a 100 W Ozone Free Xenon Lamp and an Oriel LCS-100 solar simulator using a Metrohm Autolab Potentiostat/Galvanostat PGSTAT 128. The efficiency of cells with a particular electrolyte composition has been measured at least five times in order to ensure the reproducibility. Electrochemical impedance spectra of DSSCs were obtained by using the same Metrohm Autolab potentiostat/galvanostat PGSTAT 128N with FRA 32 M frequency response analyzer (FRA) covering the 1 MHz to 0.01 Hz frequency range under the illumination of 100 mW cm^{-2}. The ionic conductivities of the electrolytes were extracted from the electrical impedance spectroscopy measurements. In the case of liquid electrolyte, the sample was kept within a spacer sandwiched between two polished stainless-steel electrodes and the conductivity measurements were taken similarly. In order to check and compare the stability, the current density–voltage (*J–V)*

measurements of DSSCs fabricated with liquid electrolyte and nanofibre gel electrolyte were recorded at AM 1.5 (100 mW cm^{-2}) simulated sunlight radiation system (PE Cell-PEC L-01) for 1 h and also for 120 h.

3. Results and discussion

3.1 *Characterization of electrospun PVdF-HFP nanofibre membranes*

In electrospinning, there are various processing parameters such as syringe pump flow rate, the rotational speed of the drum collector, the distance between the collector and the syringe tip and applied DC voltage, which directly affect the morphology and fibre diameter of the resulting nanofibre membrane. Figure 2 depicts an SEM image of an electrospun (4 min spinning times) PVdF-HFP polymer nanofibre membrane prepared in this work showing its morphology. The membrane consists of thin nanofibres with an average fibre diameter of 80–100 nm, which provides sufficient mechanical strength and appears as an effective fibre matrix to prevent the leakage of the liquid electrolyte. Moreover, the three-dimensional network structure consists of high porosity index and numerous cross-linking points. Hence, owing to these properties the fibre membrane has the ability to retain a sufficient amount of liquid electrolyte within these pores facilitating sufficient ionic mobility within and outside the mesoporous structure.

To characterize the absorption performance of electrolyte solution by the PVdF-HFP nanofibre membrane, the electrolyte uptake '*U*' was evaluated using the following formula (1) [7, 13].

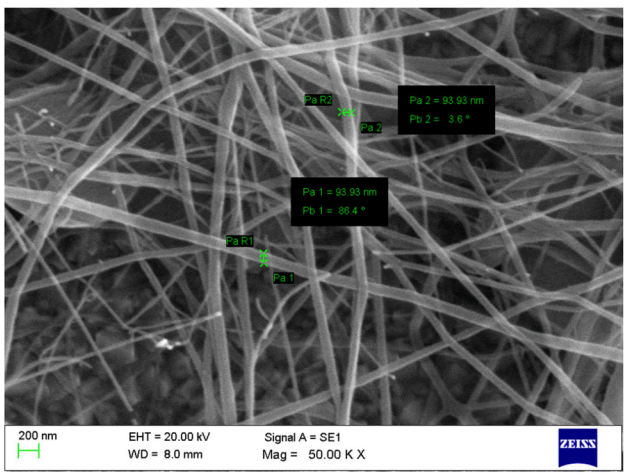

Figure 2. SEM image of a typical electrospun PVdF-HFP polymer nanofibre membrane (electrospinning time of 4 min) used in this work. The liquid electrolyte 'trapped' by this nanofibre network was used as the 'gel' electrolyte for the DSSCs. The grain-like structure seen below the nanofibre membrane in the SEM image is from the tin oxide particles in the FTO layer on the glass substrate.

$$U = \frac{m - m_o}{m_o} \times 100\%, \quad (1)$$

where m_o is the weight of the dry electrospun nanofibre membrane and m the weight of the membrane after soaking with liquid electrolyte after wiping off the excess amount of electrolyte on the surfaces of the membrane. The average liquid electrolyte uptake was recorded as 56.2% for the optimized DSSC.

3.2 *Photovoltaic performance*

The photovoltaic performance of DSSCs fabricated with PVdF-HFP nanofibre gel electrolytes prepared by varying the electrospinning time of nanofibres is shown in figure 3 and summarized in table 1. It can be seen that the maximum DSSC efficiency is obtained for the nanofibre membrane, which corresponds to the electrospinning time of 4 min. The optimized DSSC shows an efficiency of 6.79%, a short circuit photocurrent density (J_{sc}) of 12.70 mA cm^{-2}, an open circuit voltage (V_{oc}) of 801.4 mV and a fill factor (*FF*) of 66.67%. As shown in figure 3, the electrospinning time, which can be assumed to be proportional to the thickness of the nanofibre membrane, has directly affected the photocurrent density and hence the efficiency of the device. With increasing the duration of electrospinning time, the photoconversion efficiency of the DSSC gradually increased up to a maximum value and then started to decrease. The photocurrent density (J_{sc}) also exhibits the similar variation with time. Recent studies have also reported a similar correlation between the electrospinning time and photovoltaic performances [10, 13–16].

According to table 1, both maximum J_{sc} and the maximum efficiency can be observed with DSSC prepared with the electrospun polymer nanofibre membrane, which

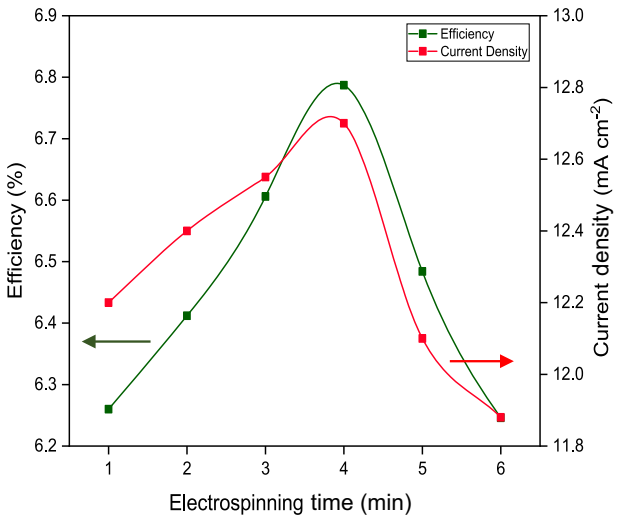

Figure 3. Variation of photoconversion efficiency and current density of electrospun PVdF-HFP nanofibre membrane-based DSSC as a function of electrospinning time.

Table 1. Photovoltaic parameters of the DSSCs made with electrospun PVdF-HFP polymer nanofibre gel electrolyte fabricated under different electrospinning times.

Electrospinning time (min)	V_{oc} (mV)	J_{sc} (mA cm^{-2})	FF (%)	Efficiency (%)
1.0	796.2	12.20	64.48	6.26
2.0	800.5	12.40	64.60	6.41
3.0	801.1	12.55	65.70	6.61
4.0	801.4	12.70	66.67	6.79
5.0	800.2	12.10	65.97	6.48
6.0	796.5	11.88	65.96	6.25

Table 2. Photovoltaic parameters of the optimized DSSCs based on liquid electrolyte and PVdF-HFP polymer nanofibre gel electrolyte (4 min electrospinning time) having the same electrolyte composition.

Electrolyte	V_{oc} (mV)	J_{sc} (mA cm^{-2})	FF (%)	Efficiency (%)
Liquid	796.3	13.36	68.36	7.28
PVdF-HFP nanofibre gel	801.4	12.70	66.67	6.79

corresponds to an electrospinning time of 4 min. When the duration of electrospinning time is low, the thickness of the fibre membrane is low, and the porosity in the fibre matrix is also expected to be low. Therefore, the liquid electrolyte uptake by the fibre matrix is also low in the thinner film, and it causes for a comparatively low rate of dye regeneration [17]. When increasing the electrospinning time, the thickness of the nanofibre membrane is increased proportionately, along with the porosity and cross-linking points. Hence, the nanofibre membrane is capable of penetrating a high amount of liquid electrolyte, thereby availing high I_3^-/I^- ions, which provide sufficient electrons for the dye regeneration, so that the device can reach the highest photocurrent density (J_{sc}) of 12.70 mA cm^{-2} and hence the maximum efficiency of 6.79%.

After reaching the maximum performance at 4 min of electrospinning time, the photocurrent density and the efficiency start to drop gradually, evidently due to the higher thickness of the nanofibre membrane. This is very likely due to the reduced mobility of iodide ions (I^-/I_3^-) within the electrolyte caused by the blocking effect imposed by the presence of more nanofibres (or higher nanofibre density) in the medium, which reduces the mobility of iodide ions [8]. Another contribution to this effect may be due to the possibility of nanofibres masking a larger area of the photoanode, thereby effectively reducing the number of photoelectrons participating in the redox reactions at the photoanode/electrolyte interface. This phenomenon gives the lowest efficiency of 6.25% and the lowest J_{sc} of 11.88 mA cm^{-2} at 6 min of electrospinning time.

A comparison of photocurrent density *vs*. voltage (*J*–*V*) curves for DSSCs fabricated with liquid electrolyte and PVdF-HFP polymer nanofibre-based gel electrolyte is shown in table 2 and figure 3. As seen from table 2, the J_{sc} value and the efficiency value obtained for the DSSC made with PVdF-HFP nanofibre gel electrolyte are somewhat lower compared to those obtained for the DSSC made with the liquid electrolyte having the same electrolyte composition. This has to be expected as the presence of the nanofibre membrane would lower the ionic mobility in the nanofibre gel electrolyte due to effective 'viscous nature' of the medium and the blocking action imposed by the nanofibre matrix. This would eventually lead to a decrease

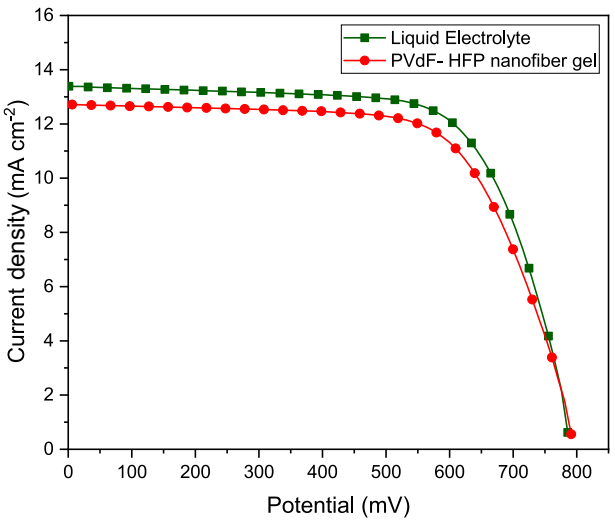

Figure 4. Photocurrent–voltage curves for DSSCs made with liquid electrolyte and electrospun PVdF-HFP nanofibre membrane gel electrolyte fabricated for 4 min of electrospinning time.

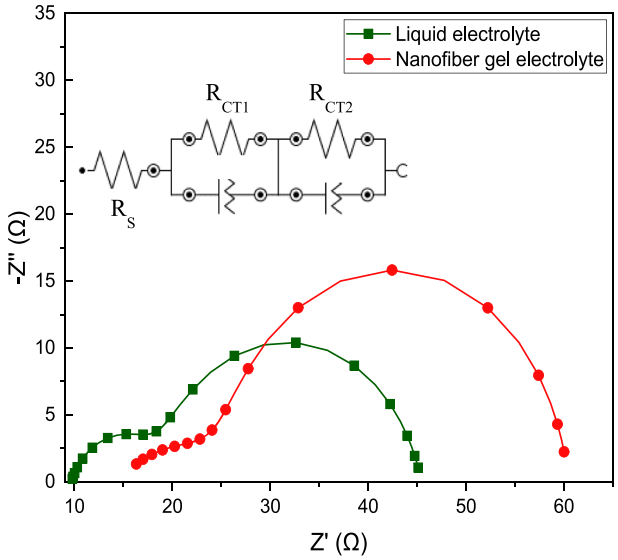

Figure 5. Nyquist plots of the DSSCs made with liquid electrolyte and electrospun PVdF-HFP nanofibre gel electrolyte.

in the photocurrent density and hence the DSSC efficiency. Figure 4 compares the photocurrent–voltage curves for DSSCs made with liquid electrolyte and electrospun PVdF-HFP nanofibre membrane-based gel electrolyte fabricated with 4 min of electrospinning time.

Moreover, liquid electrolyte-based DSSCs exhibit relatively low V_{oc} values compared to the DSSCs made with nanofibre membrane gel electrolyte. For a typical DSSC under illumination, V_{oc} is defined as the difference between the Fermi level of the TiO_2 semiconductor and the redox level of the electrolyte under an open circuit [18]. In liquid electrolyte-based DSSCs, the cations in the electrolyte, such as Pr_4N^+ and K^+, get adsorbed into the TiO_2 surface creating a positive shift of the conduction band of TiO_2, thereby causing a faster electron transfer dynamics at the TiO_2/dye interface resulting in enhanced J_{sc} at the expense of reducing the V_{oc} [12].

PVdF-HFP is a polymer with hydrophobic nature, and it generally reduces the ionic mobility of both anions (I^-/I_3^-) and cations (Pr_4N^+ and K^+) in the liquid electrolyte through the polymer membrane, thus reducing the photocurrent density [8]. Also, the PVdF-HFP nanofibre membrane in the gel electrolyte reduces the effective surface area of the photoanode exposed to the liquid electrolyte (masking effect), thereby reducing the number of adsorbed cations (Pr_4N^+ and K^+) to the TiO_2 surface, thus reducing the positive band shift mentioned above compared to the liquid electrolyte-based DSSC. This would lead to a relatively higher V_{oc} value than liquid electrolyte-based DSSC. This enhancement of V_{oc} value in DSSCs with PVdF-HFP nanofibre gel electrolyte would, in turn, decrease the value of J_{sc} due to the reduction of the rate of electron injection process at the TiO_2/gel electrolyte interface [10, 14].

3.3 *Electrochemical impedance spectroscopy*

Electrochemical impedance spectroscopy was performed in order to understand the effect of nanofibre on the charge transfer ability of the DSSCs. The Nyquist plots of the DSSCs fabricated with liquid electrolyte and PVdF-HFP nanofibre gel electrolyte are shown in figure 5, and the equivalent circuit model used is shown in the inset in figure 5.

The parameters R_S, R_{CT1} and R_{CT2} represent the series resistance, the charge transfer resistance of the Pt/electrolyte interface and the charge transfer resistance of the TiO_2/electrolyte interface, respectively. The calculated values of the equivalent circuit model corresponding to DSSCs based on liquid electrolyte and PVdF-HFP polymer nanofibre gel electrolyte are tabulated in table 3.

According to the values shown in table 3, all the charge transfer resistance values that correspond to cells based on PVdF-HFP polymer nanofibre gel electrolyte are higher than those for the cells fabricated with the liquid electrolyte. The higher values of resistance in the nanofibre gel electrolyte-based DSSC indicate that charge transport at the interfaces and in bulk are lower compared to the DSSCs fabricated with the liquid electrolyte. This phenomenon occurs with the presence of the PVdF-HFP nanofibre membrane, which reduces the mobility of iodide ions and the lower dye regeneration rate, which in turn limits the supply of I^-/I_3^- ions to shuttle between the TiO_2 electrode and the Pt counter electrode [10, 13].

Charge transfer process of DSSCs with liquid electrolyte and PVdF-HFP nanofibre gel electrolyte can be explained using the Bode phase plots shown in figure 6. The electron lifetime (τ) within the TiO_2 photoanode was determined by the maximum angular frequency (ω_{max}) of the impedance semicircle arc at middle frequencies. Table 3 shows the maximum frequency peak (f_{max}) values and the corresponding electron lifetime (τ) values in the DSSCs with each electrolyte calculated by using the following equation (2).

$$\tau = \frac{1}{\omega_{max}} = \frac{1}{2\pi f_{max}} \tag{2}$$

For the DSSC with PVdF-HFP nanofibre gel-based electrolyte, the mid-frequency peak shifted to a lower frequency, indicating a high electron lifetime (τ). The electron lifetime for DSSC made with nanofibre gel electrolyte is 11.34 ms, and for the DSSC made with liquid electrolyte, the electron lifetime is 6.30 ms. According to the literature, electron lifetime is related to the charge transfer at TiO_2/-electrolyte interface [19–21]. The higher value for the electron lifetime for the gel electrolyte-based cell may be interpreted as due to the screening effect caused by the nanofibres in contact with the TiO_2 surface, which helps reduce recombination between the mesoporous TiO_2 and the I_3^- ions [19]. This electron screening reduces the effective rate of photo-injected electrons in the TiO_2

Table 3. The series resistance (R_S) and charge transfer resistance (R_{CT}) in DSSCs fabricated with the liquid electrolyte and electrospun PVdF-HFP nanofibre membrane gel electrolyte.

Electrolyte	R_S (Ω)	R_{CT1} (Ω)	R_{CT2} (Ω)	f_{max} (Hz)	τ (ms)
Liquid	9.70	8.99	26.80	25.27	6.30
PVdF-HFP nanofibre gel	14.40	12.60	33.50	14.04	11.34

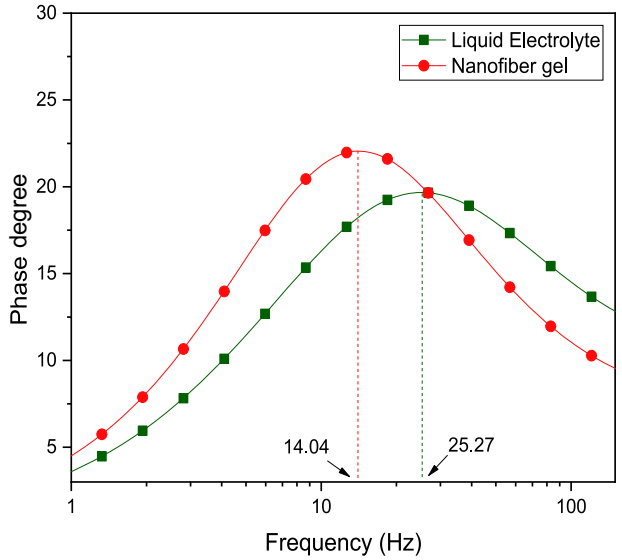

Figure 6. Bode phase plots of the DSSCs made with liquid electrolyte and electrospun PVdF-HFP nanofibre membrane gel electrolyte.

conduction band reaching the interface and undergoing reduction of I_3^- ions in the electrolyte, thereby passivating the TiO_2 and leading towards a reduction in the back transfer of electrons [22].

3.4 *IPCE measurements*

Incident photon conversion efficiency (IPCE) of a solar cell is defined as the number of electrons generated through an external circuit under short circuit conditions per incident photon [23]. In order to further substantiate the explanations given earlier, IPCE measurements were taken for the two types of DSSCs, and the two IPCE spectra are shown in figure 7. The DSSC fabricated with liquid electrolyte exhibits a little higher $IPCE_{max}$ value of 48.40% at 526 nm compared to the $IPCE_{max}$ values of 46.95% at 527 nm obtained for the DSSC fabricated with PVdF-HFP polymer nanofibre gel electrolyte. The slightly lower $IPCE_{max}$ value in the DSSC made with the nanofibre gel electrolyte may have caused due to lower photocurrent density in the nanofibre gel electrolyte-based DSSC [23]. Both IPCE curves show the broad IPCE peak range from 500 to 550 nm. These observations show that the performance of the polymer gel electrolyte-based DSSC is only slightly lower compared to the liquid electrolyte-based DSSC [10].

3.5 *Ionic conductivity analysis*

The ionic conductivity (σ) of the liquid electrolyte and PVdF-HFP quasi-solid-state gel electrolyte used for the fabrication of DSSCs was measured using the configuration, stainless steel/electrolyte/stainless steel at different temperatures from 25 to 65°C. The results are shown in figure 8 and table 4.

The liquid electrolyte exhibits a higher ionic conductivity of 11.69×10^{-3} S cm^{-1} at 25°C, whereas the PVdF-HFP quasi-solid-state nanofibre gel electrolyte exhibits an ionic conductivity of 7.16×10^{-3} S cm^{-1} at 25°C. In both these electrolytes, as expected, the conductivity gradually increases with increasing of temperature from room temperature of 25 to 65°C. The linear variation of $\ln(\sigma T)$ *vs.* $1/T$ for both these electrolytes implies that the conductivity of electrolytes follows the Arrhenius behaviour (equations 3 and 4).

$$\sigma T = Be^{-\frac{E_a}{kT}} \tag{3}$$

$$\ln\sigma T = -\frac{E_a}{k}\frac{1}{T} + \ln B \tag{4}$$

where σ is the ionic conductivity, E_a the activation energy, B the pre-exponential factor, k the Boltzmann constant and T temperature in Kelvin.

Generally, the gel polymer electrolytes, made up by soaking the polymer nanofibre membrane in a liquid electrolyte, exhibit a lower ionic conductivity compared to the corresponding liquid electrolyte, but a higher conductivity compared to a solid polymer electrolyte. Such polymer nanofibre gel electrolytes are expected to possess the combined physical properties of the liquid phase as well as the solid phase [24]. As mentioned earlier, the polymer nanofibre membrane has a uniform interwoven network structure, which consists of a high porosity index and numerous physically cross-linked points. Therefore, the nanofibre membrane structure is capable of retaining a large amount of the liquid electrolyte exhibiting a gel-like behaviour.

The activation energy for ionic motion in the two electrolytes was calculated from the gradients of the linear graphs in figure 8 and the values are 0.045 ± 0.001 eV and

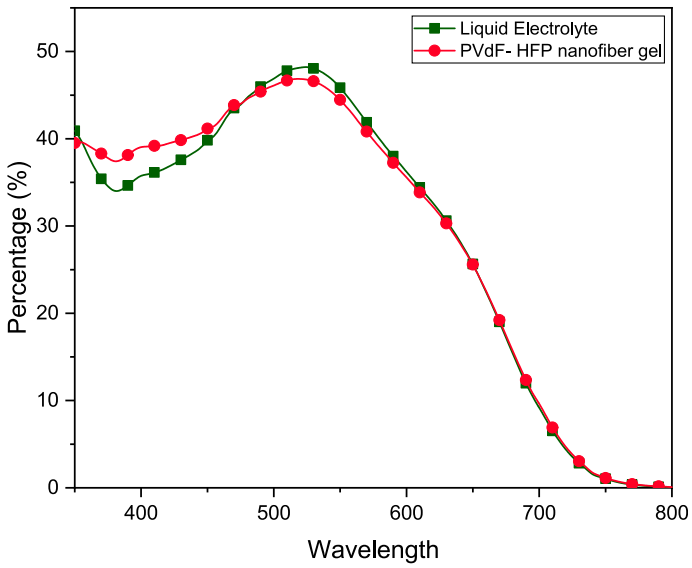

Fig. 7. IPCE spectra of the DSSCs made with liquid electrolyte and electrospun PVdF-HFP nanofibre membrane gel electrolyte.

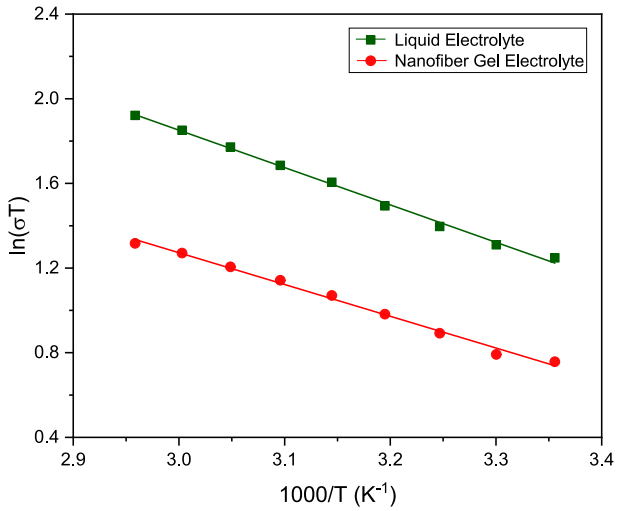

Figure 8. The variation of $\ln(\sigma T)$ plotted against the reciprocal temperature for the liquid electrolyte and the PVdF-HFP nanofibre gel electrolyte.

0.039 ± 0.001 eV for the liquid electrolyte and PVdF-HFP quasi-solid-state gel electrolyte, respectively. This lower activation energy of the gel electrolyte can be attributed to the possibility of fast ion conducting pathways introduced by the nanofibre matrix. Polymer nanofibres can provide a 3D framework structure that provides migration channels for iodide ion transport [25].

3.6 *Stability studies*

Stability studies were carried out to investigate the short-term stability and long-term stability of the optimized cell

Table 4. Ionic conductivity *vs.* temperature for the liquid electrolyte and PVdF-HFP nanofibre gel electrolyte used to fabricate the DSSCs.

	Conductivity (σ) S cm^{-1}	
Temperature (°C)	Liquid electrolyte	PVdF-HFP nanofibre gel electrolyte
25	11.69×10^{-3}	7.16×10^{-3}
30	12.22×10^{-3}	7.29×10^{-3}
35	13.12×10^{-3}	7.92×10^{-3}
40	14.23×10^{-3}	8.53×10^{-3}
45	15.66×10^{-3}	9.17×10^{-3}
50	16.69×10^{-3}	9.69×10^{-3}
55	17.93×10^{-3}	10.18×10^{-3}
60	19.11×10^{-3}	10.69×10^{-3}
65	20.27×10^{-3}	11.04×10^{-3}

prepared with the liquid electrolyte and with PVdF-HFP quasi-solid-state gel electrolyte. The efficiencies of freshly fabricated cells were measured using J_{sc} and V_{oc} values initially for 1 h and then the performance of the same cells were continuously monitored over 120 h. Figure 9a shows the efficiency *vs.* time variation during the first hour of the prepared cells. Initially the efficiency values started from a lower value and reached equilibrium values and remain essentially unchanged during the first 60 min.

Figure 9b shows the efficiency *vs.* time variation of cells over 120 h. Accordingly, the efficiency of the liquid electrolyte-based cell have degraded rapidly and after 120 h, it has retained only 44.46% efficiency of its initial value. The cell fabricated with the nanofibre gel electrolyte, on the

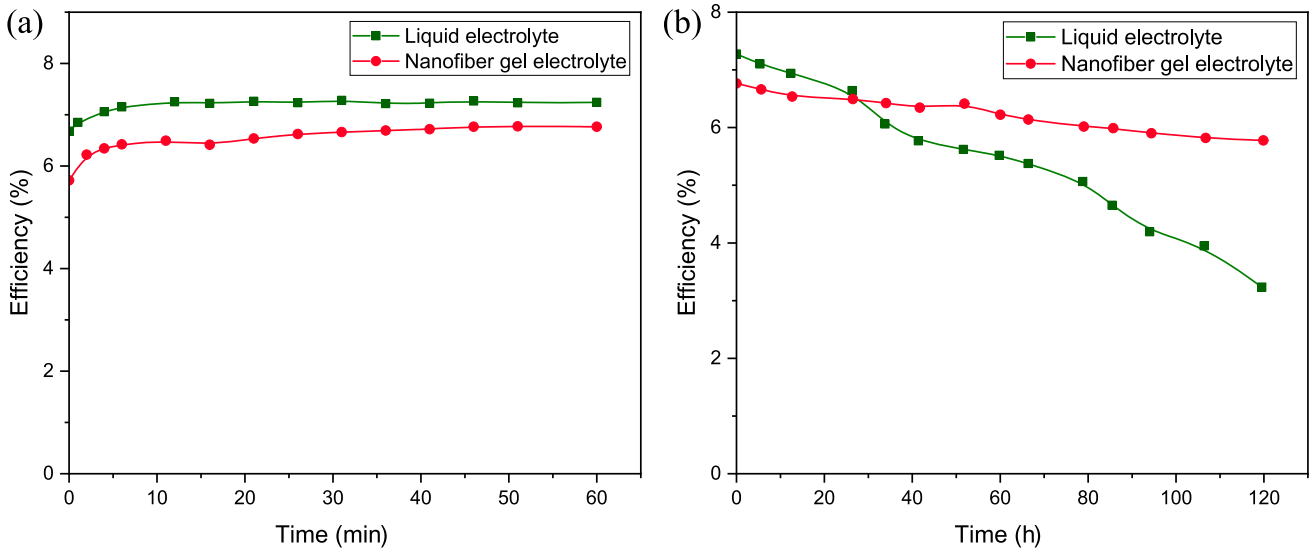

Figure 9. Stability comparison of the DSSCs fabricated with liquid electrolyte and electrospun PVdF-HFP nanofibre membrane gel electrolyte: (**a**) short-term efficiency variation over 1 h and (**b**) long-term efficiency variation over 120 h.

other hand, has shown a slower decay of efficiency and its efficiency has retained 85.40% even after 120 h. The relatively better stability of the cell fabricated with nanofibre gel electrolyte can be attributed to the 'quasi-solid' or 'gel' nature of the electrolyte formed by trapping of the liquid electrolyte within the 3D nanofibre network, thus minimizing the leakage and evaporation of the electrolyte from the edges of these 'unsealed' solar cells. These results clearly confirm that the nanofibre gel electrolyte-based DSSC is more stable compared to the liquid electrolyte for DSSC applications [26–29].

4. Conclusion

In this study, quasi-solid-state DSSCs were successfully fabricated using electrospun PVdF-HFP polymer nanofibre membrane. The SEM images show that the thin nanofibre membranes consist of nanofibres of diameter 80–100 nm with a three-dimensional chambered network structure, consisting of high porosity index and numerous physical cross-linking points facilitating the penetration and uptake of sufficient amount of liquid electrolyte to form the gel electrolyte. The average liquid electrolyte uptake was calculated to the DSSC, which offers the highest efficiency and it was recorded as 56.2%. The variation of photovoltaic performance of electrospun PVdF-HFP nanofibre membrane-based DSSCs was studied as a function electrospinning time. The short circuit current density (J_{sc}) and light-to-electricity conversion efficiency (η) have shown almost similar variations with the time duration of electrospinning. Both parameters have gradually increased to a maximum value and then decreased with the electrospinning time. Maximum efficiency of 6.79% was obtained for the nanofibre membrane electrospun for 4 min and the corresponding V_{oc}, J_{sc} and FF were 801.4 mV, 12.70 mA cm^{-2} and 66.67%, respectively. In addition, photovoltaic parameters of these optimum solar cell's performances were compared with those of an identical cell, but based on a liquid electrolyte with similar composition, exhibiting an efficiency of 7.28%. Moreover, according to the results of electrochemical impedance spectroscopy and Bode plot measurements, the incorporation of the PVdF-HFP nanofibre membrane has reduced the ion motilities in the DSSC by increasing the resistance values, although the electron lifetime has increased compared to the liquid electrolyte-based DSSC. PVdF-HFP nanofibre gel electrolyte has shown an ionic conductivity of 7.16×10^{-3} S cm^{-1} at room temperature (25°C), while, as expected, the liquid electrolyte has shown a higher ionic conductivity of 11.69×10^{-3} S cm^{-1} at the same temperature. Preliminary stability study indicates that the applicability of nanofibre membranes to DSSC provides better long-term stability by retaining 85.40% of its initial efficiency after 120 h, whereas the liquid electrolyte-based cell has retained only 44.46%. Therefore, this study shows that the nanofibre gel electrolyte offers relatively higher DSSC conversion efficiencies close to that of their liquid electrolyte counterparts, while suppressing some of the major drawbacks of liquid electrolyte-based solar cells.

Acknowledgements

We gratefully acknowledge the financial support provided by the Swedish Research Council, Dnr. 2021-04889, under the Swedish Research Links Network grant for collaborative research on solar cells between Sweden, Sri Lanka, India and Nigeria, and the Open University of Sri Lanka for support for SEM imaging.

References

[1] Chigome S and Torto N 2011 *Anal. Chim. Acta* **706** 25
[2] Shi X, Zhou W, Ma D, Ma Q, Bridges D and Ma Y 2015 *J. Nanomater.* **16** 122
[3] Wang X and Hsiao B S 2016 *Curr. Opin. Chem. Eng.* **12** 62
[4] Huang Z M, Zhang Y, Kotaki M and Ramakrishna S 2003 *Sci. Technol.* **63** 2223
[5] Gong J, Sumathy K, Qiao Q and Zhou Z 2017 *Renew. Sustain. Energy Rev.* **68** 234
[6] O'Regan B and Grätzel M 1991 *Nature* **353** 737
[7] Park S H, Won D H, Choi H J, Hwang W P, Jang S I, Kim J H *et al* 2011 *Sol. Energy Mater. Sol. Cells* **95** 296
[8] Priya A R S, Subramania A, Jung Y S and Kim K J 2008 *Langmuir* **24** 9816
[9] Thomas M and Rajiv S 2019 *New J. Chem.* **43** 4444
[10] Dissanayake M A K L, Divarathne H K D W M N R, Thotawatthage C A, Dissanayake C B, Senadeera G K R and Bandara B M R 2014 *Electrochim. Acta* **130** 76
[11] Bandara T M W J, Weerasinghe A M J S, Dissanayake M A K L, Senadeera G K R, Furlani M, Albinsson I *et al* 2018 *Electrochim. Acta* **266** 276
[12] Dissanayake M A K L, Umair K, Senadeera G K R and Kumari J M K W 2021 *J. Photochem. Photobiol. A: Chem.* **415** 113308
[13] Cheng F, Ou Y, Liu G, Zhao L, Dong B, Wang S *et al* 2019 *J. Nanomater.* **9** 783
[14] Arof A K, Aziz M F, Noor M M, Careem M A, Bandara L R A K, Thotawatthage C A *et al* 2014 *Int. J. Hydrog. Energy* **39** 2929
[15] Dissanayake M A K L, Sarangika H N M, Senadeera G K R, Divarathne H K D W M N R and Ekanayake E M P C 2017 *J. Appl. Electrochem.* **47** 1239
[16] Lee J-K, Choi H-J, Park S-H, Won D-H, Park H-W, Kim J-H *et al* 2010 *Mol. Cryst. Liq. Cryst.* **519** 234
[17] Dissanayake S S, Dissanayake M A K L, Seneviratne V A, Senadeera G K R and Thotawatthage C A 2016 *Mater. Today: Proc.* **3** S104
[18] Hamann T W, Jensen R A, Martinson A B F, Ryswyk H V and Hupp J T 2008 *Energy Environ. Sci.* **1** 66
[19] Chou H T, Hsu H C, Lien C H and Chen S T 2015 *Microelectron. Reliab.* **55** 2174
[20] Gao Z, Yang J, Cheng Q, Tian L, Jiang K and Yang L 2013 *Mater. Chem. Phys.* **137** 866
[21] Tang X, Wang Y and Cao G 2013 *J. Electroanal. Chem.* **694** 6
[22] Khan A A, Kamarudin M A, Qasim M M and Wilkinson T D 2017 *Electrochim. Acta* **244** 162
[23] Gnana G, Balanay M P, Nirmala R, Kim D H, Kumar T R, Senthilkumar N *et al* 2016 *J. Nanosci. Nanotechnol.* **16** 581
[24] Tripathi S K, Gupta A and Kumari M 2012 *Bull. Mater. Sci.* **35** 969
[25] Liu W, Lee S W, Lin D, Shi F, Wang S, Sendek A D *et al* 2003 *Nat. Energy* **17035** 1
[26] Xue G, Guo Y, Yu T, Guan J, Yu X, Zhang J *et al* 2012 *Int. J. Electrochem. Sci.* **7** 1496
[27] Angaiah S, Murugadoss V, Arunachalam S, Panneerselvam P and Krishnan S 2018 *Eng. Sci.* **4** 44
[28] Thomas M and Rajiv S 2020 *Electrochim. Acta* **341** 136040
[29] Sahito I A, Ahmed F, Khatri Z, Sun K C and Jeong S H 2017 *J. Mater.* **52** 13920